Analysis and Comparison of Unconventional Converters for Switched Reluctance Machine Drives

Afzal Ahammed Shaik[1], Arjun S[2], Lenin N.C[3]*
1- Department of Electrical Engineering, VIT Chennai, Chennai, India.
Email: afzalshaik1993@gmail.com
2- Department of Electrical Engineering, VIT Chennai, Chennai, India.
Email: afzalshaik1993@gmail.com
3- Department of Electrical Engineering, VIT Chennai, Chennai, India.
Email: lenin.nc@vit.ac.in (Corresponding author)

Received: February 2018 Revised: May 2018 Accepted: June 2018

ABSTRACT:
Proliferation of electronics is a major breakthrough in the industrial sector as these play a promising role in the functioning of electric machines and together described as an electric drive. In this regard, the important factor is the efficiency of the electric drive. Based on this aspect, many electric machines have been invented and among all those machines switched reluctance motor (SRM) has found to be more beneficial because of its reduced losses. This paper presents different unconventional converters which are helpful for the functioning of low power SRM drives. Three different converters along with simulation results are presented and based upon the results of the three converters, the efficient converter for low power SRM drives is chosen for the hardware development. Experimental tests and simulations have shown the proposed converter results are closely correlated with the simulated results.

KEYWORDS: PIC Micro Controller, Split DC Converter, H-Bridge Converter, Shared Switch Converter, Switched Reluctance Machine (SRM).

1. INTRODUCTION

Switched Reluctance Machines (SRM) has been playing a very prominent role and are considered to be the most potential candidates in the industrial applications for the researchers. This importance of SRM in the applications is made possible because of the day to day improvement in power electronics [1]. SRM has windings only on the stator pole and the rotor is made with salient steel with no windings on it. This results in decreasing the conduction losses of the machine, and consequently, increased efficiency and reduced cost. Another major factor is controlling the torque ripple, in order to overcome this factor many converters were developed [2-6]. The construction of the SRM is very simple and rugged and is suitable for ultra-high speed applications. It is also called as a double salient motor as the stator and rotor have salient poles, and produces unidirectional torque. The most promising about this motor is independent phase control, that is, even during its functioning if any of the phase winding gets damaged, the remaining phases could be able to take over the control [3-10]. This independent phase control of the SRM leads to the necessity of the converter for its operation. It cannot be operated by using the direct supply mains, the voltage from the power source must be greater than the back emf generated in the phase windings in order to get high currents at high speeds.

For the efficiency of the drive ,both the converter and motor must satisfy their own conditions. The conditions that an SRM converter must satisfy are as follows: [11-13]

- Each phase of the SRM must be able to conduct independently besides the other phases.
- The excitation of the converter must be made before the phase of the SRM goes into magnetization or demagnetization condition
- In order to improve the efficiency, fault tolerance, high magnetization and demagnetization times, the converter should satisfy a number of requirements like thermal resistance.
- Energy during demagnetization must be restored or used for the next phase and phase overlap control must be satisfied.
- It must be able to apply high positive excitation voltage to establish a greater positive current.
- It must be able to operate in freewheeling mode and thereby reducing the switching losses.
- Reducing the demagnetization time by developing a negative voltage in a short period of time [14-16].

Based upon the above-mentioned conditions a

number of converters are developed for the functioning of SRM with high efficiency. Split DC Converter (SDDC), Shared Switch Converter (SSC) and H-Bridge Converter (HBC) which is also called as full bridge synchronous rectifier are discussed in this paper.

In this paper, section 2 explains the basic Circuit Diagram of three proposed converters with its modes of operation. Section 3 elucidates the simulation of the circuit at various loaded conditions graphically. Section 4 describes the prototype converter developed for the SRM and its results are compared with the simulation results. Section 5 concludes with the advantages and drawbacks of the converter.

Nomenclature	
e_L	Phase voltage during magnetization
L	Inductance
i	Instantaneous current
V_s	DC bus voltage
t_1	Rise time, On time
t_2	Fall time
V_c	Capacitor voltage
I_{max}	Maximum RMS current
V_s	Source voltage
V_a	Average output voltage
K	Duty ratio
$\frac{dL}{d\theta}$	Change in Inductance with respect to the position
ω_m	Speed of the machine
R_s	Stator winding resistance
V	Phase voltage

2. CIRCUIT DIAGRAM AND MODES OF OPERATION

In this section the circuit diagram and the modes of operation of the three converters HBC, SSC and SDCC, are explained: [17-18].

2.1. Circuit and Operation of HBC.

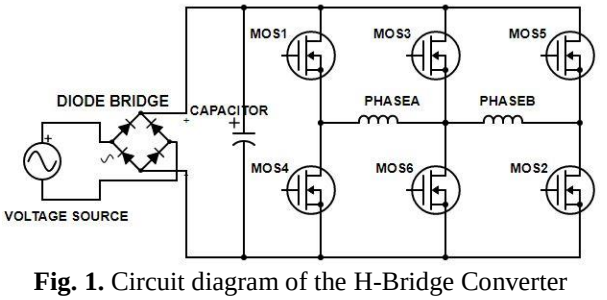

Fig. 1. Circuit diagram of the H-Bridge Converter (HBC).

The circuit of HBC consists of 6 switches for a two phase SRM. When a rectified DC is given as input magnetization of the phase A takes place with the turning of MOS1 and MOS6 to ON state, later freewheeling action takes place between MOS4 and MOS6. Later when the current value reaches its limit, demagnetization of the phaseA takes place through MOS4 and MOS3.

The circuit diagram operation can be explained in three different modes:

1. Magnetization mode
2. Freewheeling mode
3. Demagnetization mode

2.1.1. Magnetization mode

In this mode of operation, phaseA windings get excited by turning on MOS1 and MOS6. The current flows through the closed path (as shown in Fig. 2) during this mode of operation and the phaseA gets magnetized.

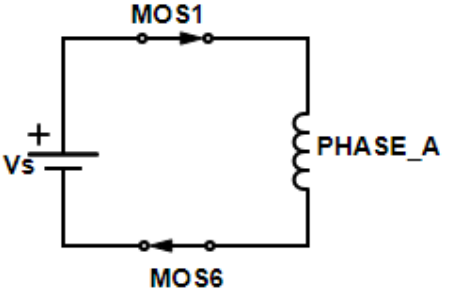

Fig. 2. Magnetization mode of HBC.

The magnetization of the phase is shown in the form of the waveform in Fig. 3. During magnetization, the voltage across the phase could be written as

$$e_L = L\frac{di}{dt} \quad (1)$$

Where L represents the phaseA and *di/dt* represents the change in the current.

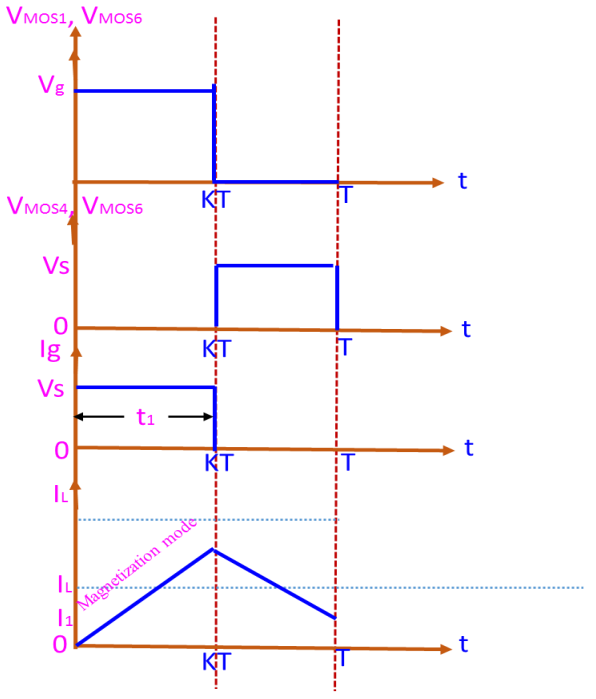

Fig. 3. Waveform representation of Magnetization Mode.

As shown in the above waveform, till the switch is in on, state the phase is in magnetization mode.

2.1.2. Freewheeling mode

In this freewheeling mode of operation MOS1 gets turned off and MOS4 is set to on state, and the MOS6 is still in on condition as shown in Fig. 4.

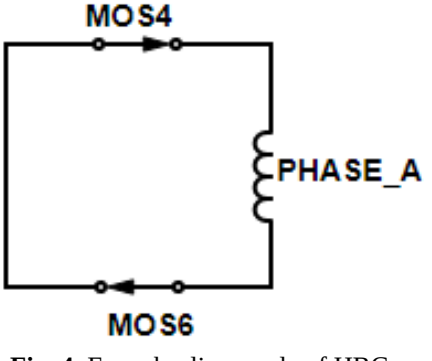

Fig. 4. Freewheeling mode of HBC.

The energy present on the phase during magnetization mode appeals to freewheel through the switches MOS4 and MOS6 till the excitation of the phase current reaches its peak value. This freewheeling action is shown in Fig. 5.

The fall time of the current can be written as

$$t_2 = \frac{\Delta IL}{V_s} \qquad (2)$$

Where ΔI represents the change in the current, L represents the Phase and Vs. represents the dc bus voltage.

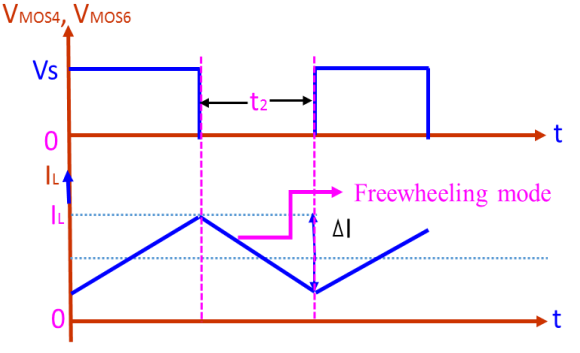

Fig. 5. Waveform representation of the Freewheeling mode of HBC.

This waveform represents that, the energy present in the phase is freewheeling between the two switches MOS4 and MOS6.

2.1.3. Demagnetization mode

In this demagnetization mode as soon as the phase current reaches its peak value, the switch MOS6 gets turned off and demagnetization happens through MOS4 PHASEA and MOS3 as shown in Fig. 6.

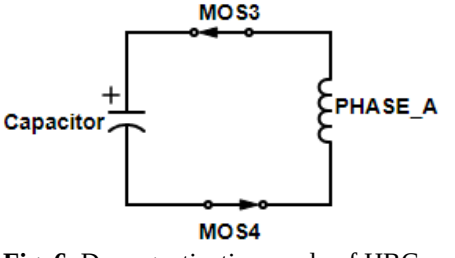

Fig. 6. Demagnetization mode of HBC.

The energy present in the phase is used for mechanical work and the remaining excess energy is fed back to the dc link capacitor where the energy is stored or utilized for the next phase. The demagnetization action is explained in a waveform shown in Fig. 7.

The voltage across the capacitor during charging that is demagnetization mode is given as

$$V_c = \frac{1}{C}\int i_c dt + V_c(\mathrm{t}=0) \qquad (3)$$

Where i_c is the capacitor current and V_c is the capacitor voltage at time zero.

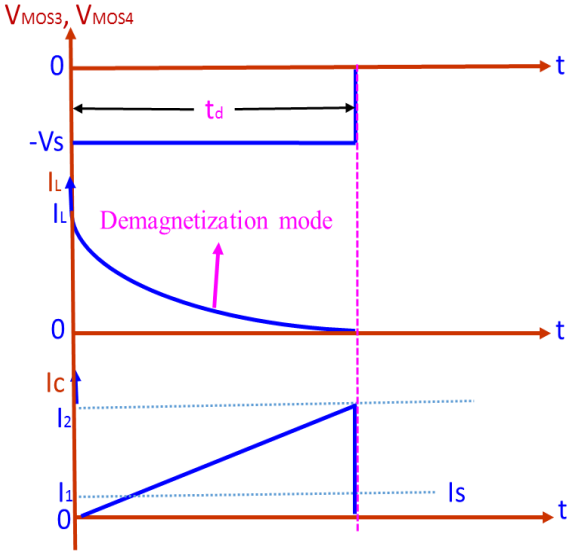

Fig. 7. Waveform representation of the Demagnetization mode of HBC.

As shown above, a negative voltage is created across the phase, resulting in the charging of the dc link capacitor. These modes of operation carry over to the next phase with a phase delay across the switching of the mosfets.

2.2. Circuit and Operation of SSC

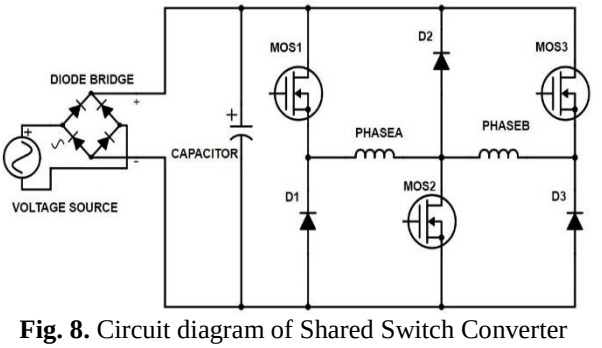

Fig. 8. Circuit diagram of Shared Switch Converter (SSC).

The working of the Shared Switch Converter is that the phaseA gets magnetized with the turning on of switches MOS1 and MOS2. Later MOS1 gets turned off and a freewheeling path is formed between the switch MOS2, phaseA and diode D1. When a current command of the phase is reached, demagnetization takes place and energy fed back to the source through the diodes which attains to be in forward biased condition.

The circuit operation can be explained in three different modes as shown below.

2.2.1. Magnetization mode

In this mode, the magnetization of phase takes place as shown in Fig. 9. A single phase AC supply is rectified into a regulated DC supply by using a full bridge rectifier in the circuit shown in the circuit diagram in Fig. 8.

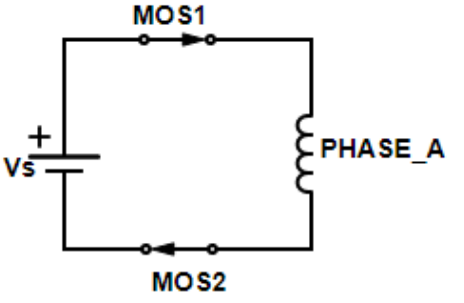

Fig. 9. Magnetization mode of SSC.

When the supply is given, the two switches MOS1 and MOS2 are in on state and MOS3 is in off condition. Diodes D1 and D2 are in reverse biased. As the switches turned on, a closed path is formed and the phase L gets excited.

During the magnetization of L, it follows the path of MOS1, L and MOS2 and thus the phase gets excited.

2.2.2. Freewheeling mode

In this mode MOS1 is in open circuit condition and freewheeling action would be taken place between the diode (D1), L and MOS2. The equivalent circuit is shown in Fig. 10.

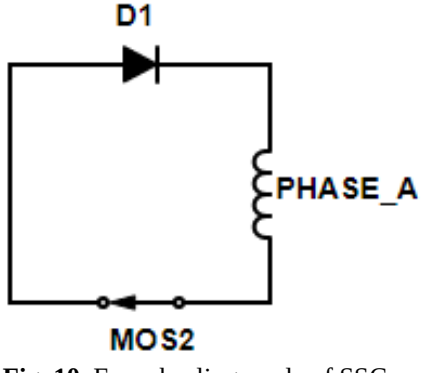

Fig. 10. Freewheeling mode of SSC.

When the phase excitation reaches to its saturation state that is when it gets completely excited, MOS1 is set to be off state and the amount of energy present in the phase freewheels through the MOS2 and D1.

Assuming a lossless circuit, the average output voltage is given as

$$V_a = V_S \frac{t_1}{T} = KV_S \quad (4)$$

Where k is called as duty cycle and the average input current is given as

$$I_s = kI_a \quad (5)$$

The path of freewheeling would be D1, L and MOS2.

2.2.3. Demagnetization mode

In this mode of operation both the switches MOS1 and MOS2 get into off condition and phase gets demagnetized. The equivalent circuit is shown in Fig. 11.

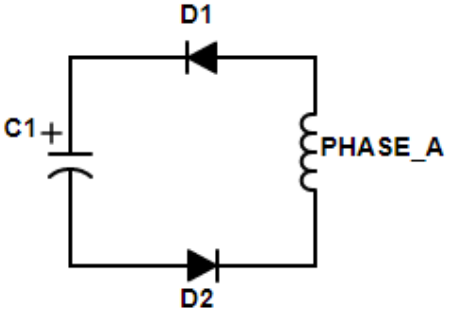

Fig. 11. Demagnetization mode of SSC.

The average capacitor current is given as

$$I_c = \frac{\Delta I}{4} \quad (6)$$

The maximum RMS current is given as

$$I_{max} = \frac{I_p}{\sqrt{2}} \quad (7)$$

Where Ip is the peak current. As the two switches MOS1 and MOS2 switch into off state and the diodes D1 and D2 gets forward biased, the energy in the phase is useful to do the mechanical work. The excess energy present in the phase freewheels back to the source through the diodes, thus energizing the capacitor.

The same principle of operation is carried out in the next alternate phase that is PHASEB with respect to the circuit diagram shown in Fig. 8 where MOS2 and MOS3 would be on and MOS1 is set into OFF state and the modes of operation repeats as illustrated in Figs 9, 10 and 11.

2.3 Circuit and Operation of SDCC

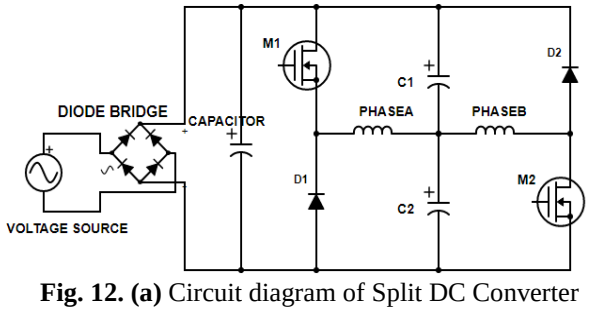

Fig. 12. (a) Circuit diagram of Split DC Converter (SDDC).

The working of the Split DC Converter is carried out in such a way that the magnetization of the phaseA takes place with the turn on switch MOS1. Later as the switch gets into the off state, demagnetization of the phaseA takes place and the energy obtained during demagnetization is stored in the capacitor C2.

The circuit operation is carried out in two different modes of operation

A. Magnetization
B. Demagnetization

2.3.1. Magnetization mode

In this mode of operation, when the supply which is converted from AC to DC is given to the circuit the switch M1 gets into on state and the phase A gets excited. Thus forming a closed path between switch M1, phase A and capacitor C1 as shown in Figs. 12.

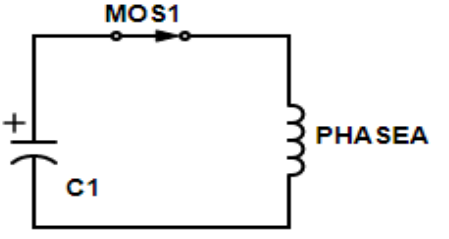

Fig. 12. (b) Magnetization mode in SDCC.

The behavior of the circuit during magnetization mode is shown in Fig. 13.

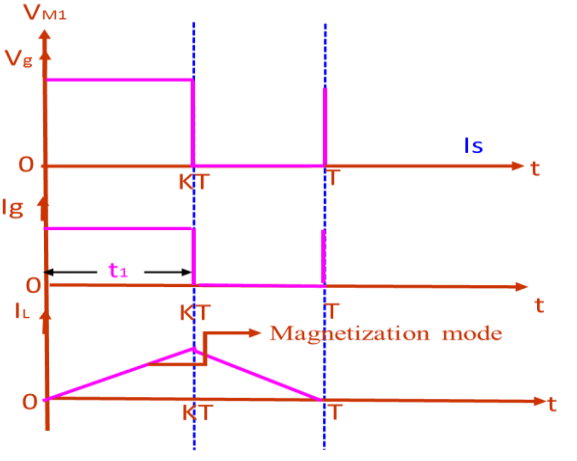

Fig. 13. Waveforms of the magnetizing mode in SDCC.

In the above Fig. 13, Vg represents the gate voltage of the switch M1, Ig represents the gate current and I_L represents the current in the phase. It can be seen that when the switch is in on state the phase inductance is getting magnetized.

2.3.2. Demagnetization mode

In this mode of operation, the energy present in the

phase gets reduced and energy from the phase flows into the capacitor C2 and the capacitor gets charged, as shown in Fig. 14.

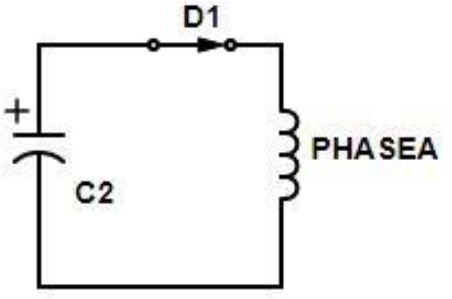

Fig. 14. Demagnetization mode in SDCC.

The behavior of the circuit during the demagnetization mode is shown in Fig. 15.

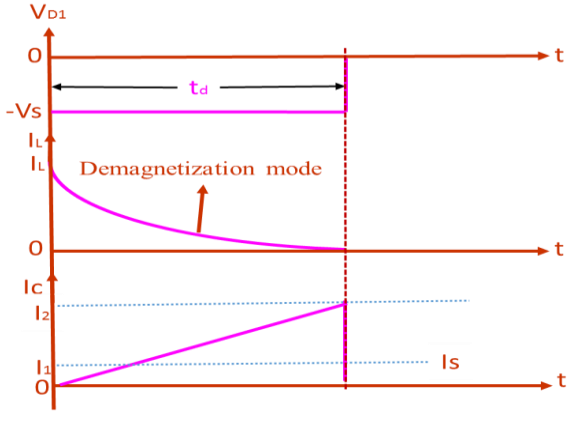

Fig. 15. Waveforms of the demagnetizing mode in SDCC.

In the above Fig.15, Vd1 represents the voltage across the diode and I_L represents the load current which is getting demagnetized. And as this happens, the voltage across the capacitor increases. That is, the capacitor is getting into the charging condition.

3. SIMULATION OF THE CONVERTERS

Before programming, the simulation of the circuit is carried out which helps understand the performance of the converter, when it undergoes a practical implementation. Simulations could be performed with many simulation software.

In this paper the simulation is carried out using PSIM software. At different loaded conditions. The specifications of all the proposed converters which are designed for 200W SRM are given in Table-1 below.

Table 1. Specifications of HBC, SSC and SDDC.

Converter	Component Name	Voltage rating	Current rating	Resistance
HBC	IRF740	400V	10A	0.48Ω
SSC	IRF740	400V	10A	0.48Ω
SDCC	IRF740	400V	10A	0.48Ω

3.1. Simulation of H-Bridge Converter.

The simulation is done by using the mosfets IRF740 because of its specifications for the rated power applications.

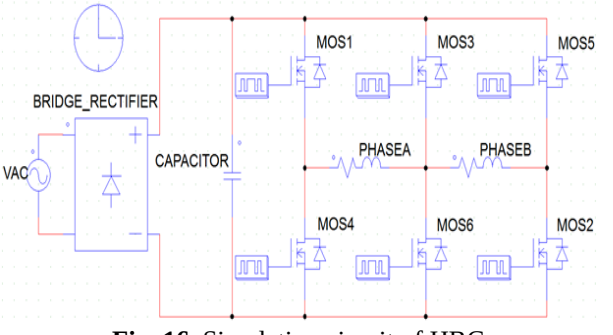

Fig. 16. Simulation circuit of HBC

The simulation of the circuit is performed at different loaded conditions and the change in the values of the currents obtained are shown in Table1. Simulations carried at 50% load and 90% load are displayed. The value of change in inductance with respect to position is taken as $\frac{dL}{d\theta} = 0.236H / rad$.

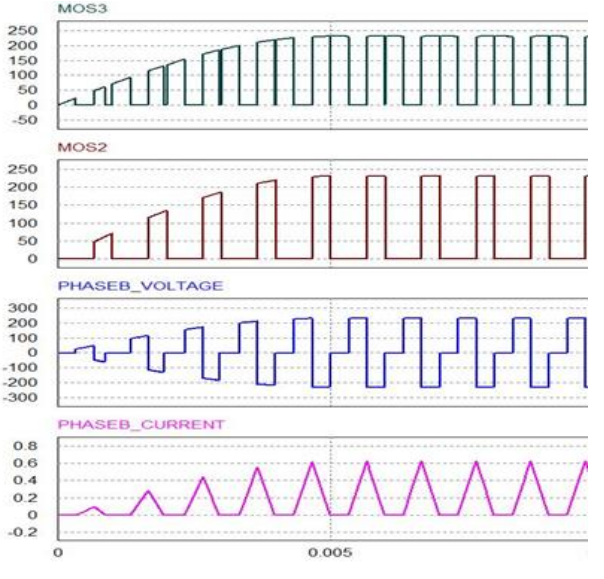

Fig. 17. The simulation result of HBC at 50% load.

The voltage equation for the Switched Reluctance Machine (SRM) is given as

$$V = IR_s + L\frac{di}{d\theta} + \omega_m i\frac{dL}{d\theta} \quad (4)$$

Where IR_s is the Resistive voltage drop, $L\frac{di}{d\theta}$ is the inductive voltage drop and $\omega_m i\frac{dL}{d\theta}$ is the induced emf.

The simulation results for different loaded conditions of HBC are shown in Table 2.

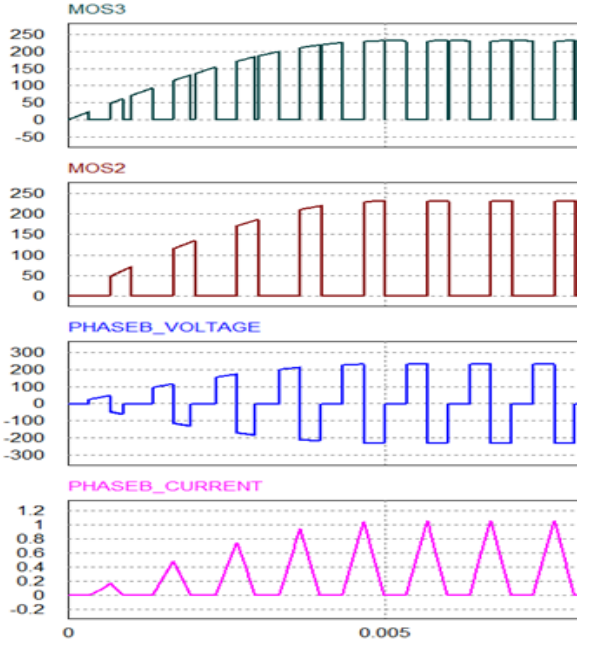

Fig. 18. Simulation result of HBC at 90% load.

For a loaded condition of 50% load, the current raising time is 0.00275seconds and the obtained phase current is 0.6A and phase voltage is 116V. Similarly, when a load of 90% is applied, phase voltage is 180V and the phase current obtained is 1A.

3.2. Simulation of Shared Switch Converter.

When an AC supply is rectified to DC and is given as input. The voltage across the switch (MOS1) is 200V.

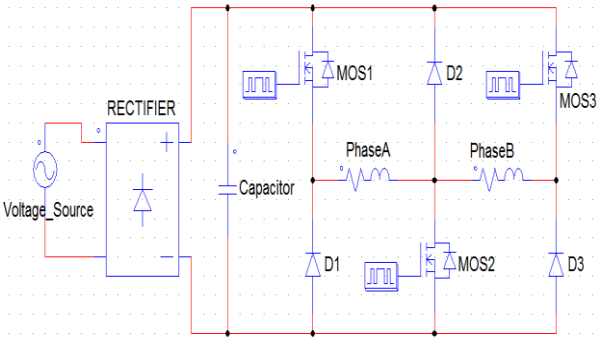

Fig. 19. Simulation circuit of SSC.

The diode voltage shown as D1_voltage is exactly opposite to that of the switch voltage according to the principle of SSC. The phase current is 1 A for a given phase voltage of 200V shown in Fig. 20.

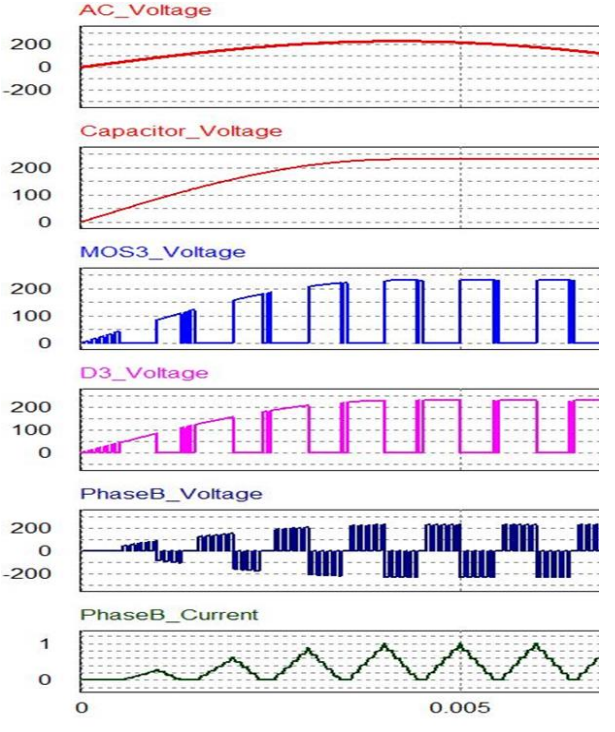

Fig. 20. Simulation result of SSC.

The simulation is carried out at different loaded conditions and the obtained results are displayed in table 2.

The simulation result at 60% load in SSC is shown below in Fig. 21.

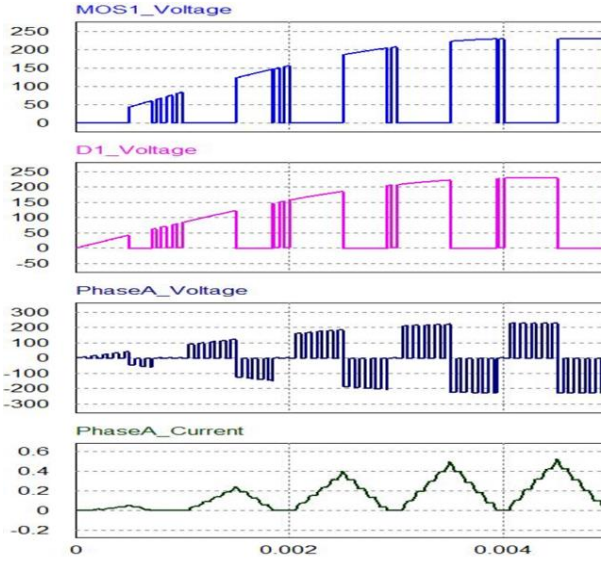

Fig. 21. Simulation result of SSC at 60% load.

The current rising time is 0.0005seconds and the obtained phase current is 0.5 Amperes and voltage is 166.3V.

3.2. Simulation of Split DC Converter.

The simulation circuit of SDCC which is carried out using PSIM software is shown below in Fig. 22.

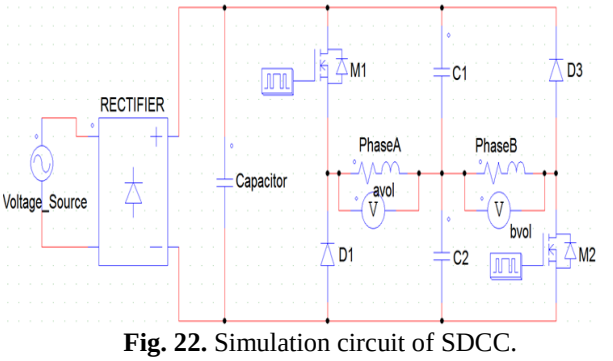

Fig. 22. Simulation circuit of SDCC.

When a rectified DC supply of 200V is applied across the switch of the converter, it gets turned on and the phaseA gets excited. The voltage across the phase gets reduced as shown in Fig. 23 below.

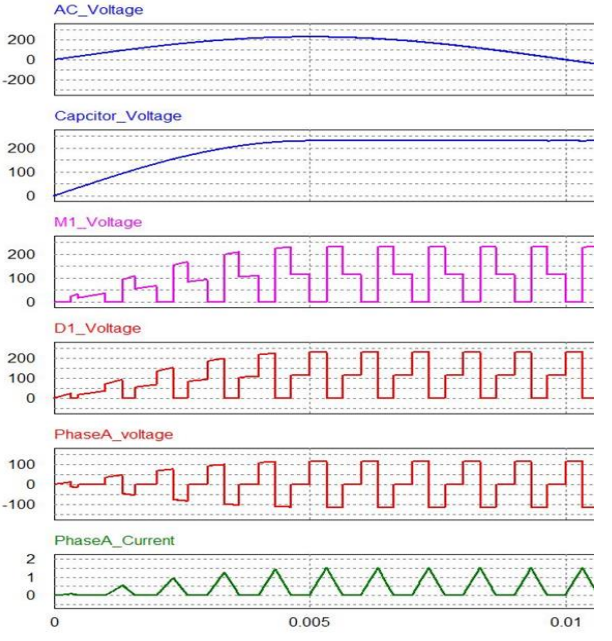

Fig. 22. Simulation result of SDCC at phaseA.

This reduction in the voltage is due to the presence of the capacitors as they try to get charged. During excitation the full voltage from the supply mains across the phase could not be utilized. The voltage across the phase appears to be 100V and the current is around 1.5A.

The simulation of the circuit is conceded for different loaded conditions and the results are shown in Table-2.

Simulation result at 50% loaded condition is shown in Fig.23.

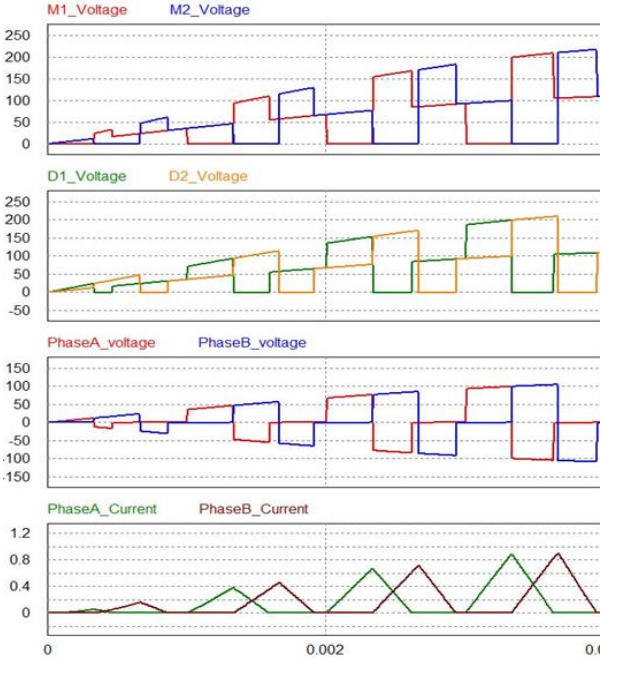

Fig. 23. Simulation result of SDCC at 50% load.

From the above Fig. 23 we can see that, for an applied voltage of 200V, the voltage across the phase is settled at 100V and the value of the current is around 1A. From the obtained results, the efficiency of the converters is calculated and the calculated efficiency is compared between the three converters.

Through further developments of the prototype, the converter has proceeded with a good efficiency.

From table 2, it can be deduced that the Split DC Converter is more efficient compared to Shared Switch Converter and H- Bridge Converter at 430Watt output power, but is less efficient at 200W output power. Graphical representation of the Output Vs. the Efficiency of all three converters is shown in Fig. 24.

Table 2. Simulation results of HBC, SSC and SDDC.

% Load	20			40			60			80			100		
Converters	SSC	SDCC	HBC	SSC	SDCC	HBC	SSC	SDCC	HBC	SSC	SDCC	HBC	SSC	SDCC	HBC
Voltage (V)	200	200	200	200	200	200	200	200	200	200	200	200	200	200	200
Current (A)	0.15	0.2	0.06	0.33	0.5	0.2	0.53	0.8	0.35	0.77	1.14	0.65	1	2.1	1.2
Output Power (W)	30	40	12	67	100	40	111	160	70	153	228	130	200	425	240
Speed (rpm)	300	300	300	500	500	500	700	700	700	1000	1000	1000	1400	1400	1400
Input Power (W)	158	181	54	176	232	114	188	275	134	239	345	200	285	537	289
Efficiency (%)	19	22	22	38	43	35	59	58	58	64	66	68	70	79	80

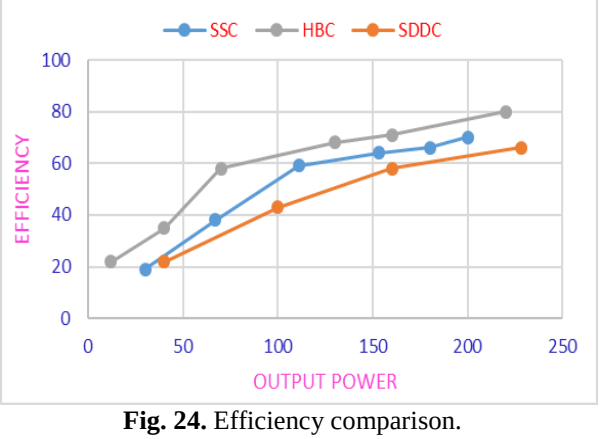

Fig. 24. Efficiency comparison.

From the above graph it can be concluded that HBC is more efficient when compared to SDDC and SSC at low power applications. Based upon this analysis a prototype has been developed for H- Bridge converter.

4. PROTOTYPE DEVELOPMENT OF HBC.

The sequential switching pulses which are required to drive the converter are generated by a controller and a driver.

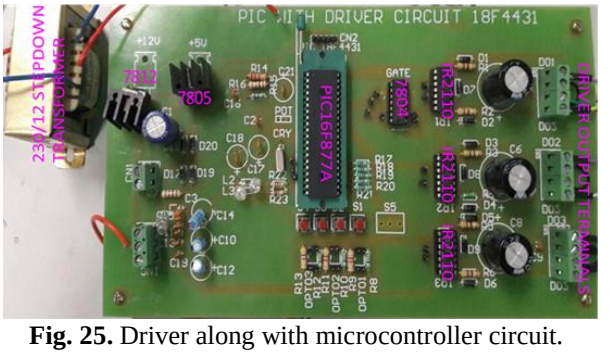

Fig. 25. Driver along with microcontroller circuit.

The above Fig. 24 shows the microcontroller and the driver circuit. PIC16F877A is used as the controller circuit in order to provide necessary pulses to the driver. IR2110 is applied as a driver circuit which helps in boosting up the pulse voltage given to the switches according to the requirement of the switch to get into on or off state in a sequential manner.

The converter prototype is shown in Fig. 26, where mosfets are used as the functioning elements of the converter and a rectifier (D35XB60) used to covert AC to DC shown in Fig. 27.

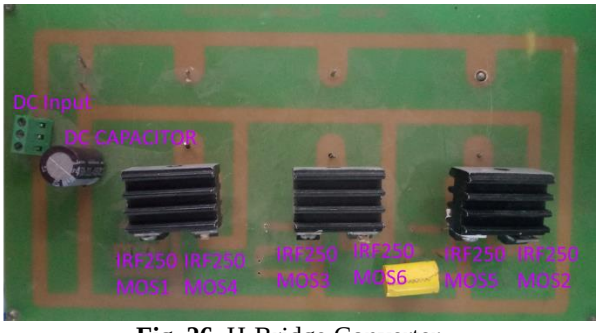

Fig. 26. H-Bridge Converter.

As shown in the above prototype of H-Bridge converter IRF250 is used as mosfet switch based upon the requirement of the power rating. Heat sinks are provided in order to protect the switches from thermal conductivity.

The input to the HBC converter is a DC supply which is obtained by rectification of an AC supply to DC using a bridge rectifier (D35XB60) and the ripples obtained are minimized using filter capacitors as shown in Fig.27.

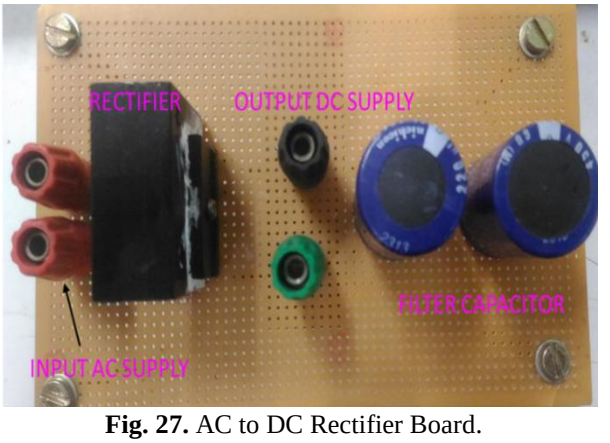

Fig. 27. AC to DC Rectifier Board.

The testing is carried out at full load value and the results obtained are displayed in Fig. 28.

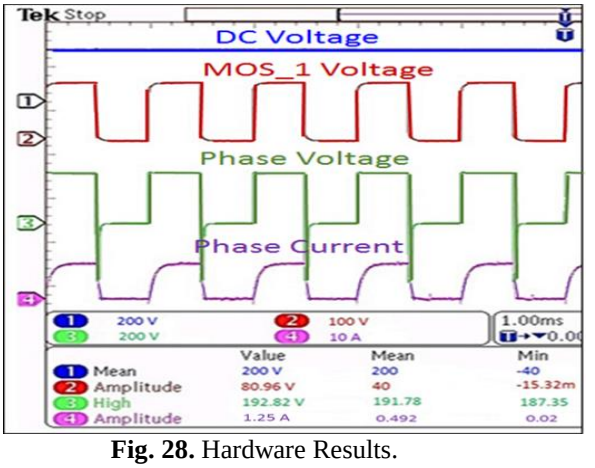

Fig. 28. Hardware Results.

As shown in the above Fig. 28, the simulation of the HBC Converter is carried at full load condition and at a given voltage of 200V, the voltage across the phase is 190V and the current obtained is around 1.25Amps.

The testing is carried for different loaded conditions and the results obtained are shown in graphical representation.

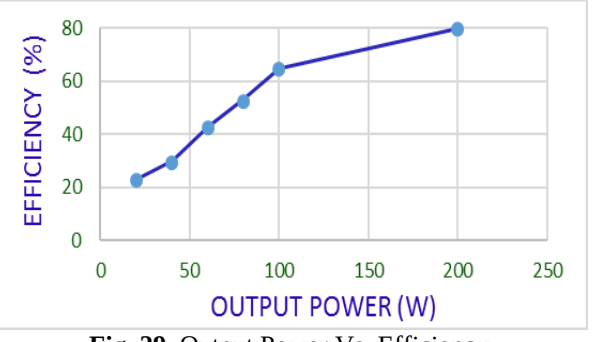

Fig. 29. Output Power Vs. Efficiency.

Based upon the test results of the drive carried over different loaded conditions, the output Vs. efficiency graph has been plotted and it can be seen that the converter functions at an efficiency of 80%.

Table 3. Advantages and drawbacks of proposed converters.

Converters	Advantages	Drawbacks
H-Bridge Converter	• Provides both generating and motoring modes of operation. • Good operational efficiency during operating and freewheeling modes. • Reduced size of the converter due to less switches.	• Provision of additional gate drive circuits due to the utilization of power switches
Shared Switch Converter	• Switches and diodes requirement is reduced. It uses only 6 switches, (3 mosfets and 3 diodes) for a two phase SRM.	• The freedom of operation is limited when compared to other converters. • A switch must be operated continuously which reduces the fault tolerance

	• Only 3 gate drive supply required. • Size of the converter is reduced when compared to other converters	• Care must be taken in order to see that any mutual inductance may not cause excessive electromotive force resulting in unwanted circulated currents.
Split DC Converter	• It achieves the capability of operating with good efficiency having a single switch per phase without adding any extra passive components and still achieves the required controllability and flexibility.	• Requirement of even number of machine phases and balancing the charge across the DC link capacitors C1 and C2, which results in some loss during the independent phase control. • The converter has less fault tolerance which causes unbalancing in the other phase connected to it. • The converter requires only even number of phases. • Reduced phase voltage that is only half of the supply voltage is applied in the phase windings during magnetization and demagnetization, decreasing in the closed loop current response and speed.

5.4. Applications of the Converters.

These converters are well suitable for low power applications of the SRM drive motors

- Flux switching machines (FSM)
- Switched Reluctance Machines (SRM)
- Flux Reversal Machines (FRM)
- DC Machines (DCM)

5. CONCLUSION

From the obtained results it can be concluded that:

- SSC converter is applicable only for low power applications. During the change in the direction of the machine, the reference speed must be kept all back to zero in order to give negative speed command.
- From the drawbacks, it can be concluded that proper care must be taken regarding the choosing of the switches for SSC.
- H- Bridge converters are applicable at low power applications since increase in the power results in increase of the switching losses of the converter.
- It is capable of generating negative DC link voltage during demagnetization which helps in restoring the energy back to the DC source or could be applied to the next phase and it has fast magnetizing and demagnetizing modes.
- Based upon the disadvantages, we can say that proper care must be taken while choosing the driver circuit which could generate necessary pulses to all the switches.
- Finally, from the test results we can say that the converter HBC is capable of functioning at 80% efficiency.
- SDDC converter is capable of operating at good efficiency using only a single switch per phase
- From the drawbacks it could be concluded that the value of the capacitors also plays a major role in determining the efficiency and variable speed applications.

REFERENCES

[1] Chun Gan, Jianhua Wu, Qingguo Sun, Shiyou Yang, Yihua Hum Lebing Jin, **"Low-cost Direct Instantaneous Torque Control for Switched Reluctance Motors with Bus Current Detection Under Soft Chopping Mode,"** *IET Power Electron*, Vol. 9, Iss. 3, pp. 482-490, 2015.

[2] A. Christopher Hudson, N. S. Lobo, R. Krishnan, **"Sensorless Control of Single Switch Based Switched Reluctance Motor Drive Using Neural Network,"** *IEEE Transactions on Industrial Electronics*, Vol. 55, Iss.1, pp. 321-329, 2008.

[3] R. Krishnan, P. Materu, **"Analysis and Design of a Low Cost Converter for Switched Reluctance Motor Drives,"** *IEEE Transactions on industrial applications*, Vol. 29, Iss.2, pp. 320-327, 1993.

[4] Jaehyuck Kim, Keunsoo Ha, R. Krishnan, **"Single Controllable Switch Based Switched Reluctance Motor Drive for Low Cost, Variable Speed Applications,"** *IEEE Transactions on Power Electronics*, Vol. 27, Iss.1, pp. 379-389, 2012.

[5] M. V. Nitesh, S. Arjun, Shaik Afzal Ahammed, P.

Ramesh, N. C. Lenin, **"Experimental Comparison of 70W Switched Reluctance Machines with Different Types of Converter Topologies,"** *1st International Conference on Power Engineering Computing and CONtrol, PECCON*, Vol. 117, pp. 306-313, 2017.

[6] Jaehyuck Kim, R. Krishnan, **"Novel Two Switch Based Switched Reluctance Motor Drive for Low Cost High Volume Applications,"** *IEEE Transactions on Industry Applications*, Vol. 45, Iss. 4, pp. 1241-1248, 2009.

[7] T. J. E. Miller, **"Electronic Control of Switched Reluctance Machines"**. Ohio, USA: Manga Physics, 2001.

[8] J. Liang, D. H. Lee, J. W. Ahn, **"Direct Instantaneous Torque Control of Switched Reluctance Machines Using 4-Level Converters,"** *IET Electric Power Applications*, Vol. 3, Iss. 4, pp. 313-323, 2009.

[9] K. Tomczewski, K, Wrobel, **"Quasi Three Level Converter for Switched Reluctance Motor Drives Reducing Current Rising and Falling Times,"** *IET Power Electronics*, Vol. 5, Iss. 7, pp. 1049-1057, 2012.

[10] H. C. Chang; C. H. Chen; Y. H. Chiang; W. Y. Sean; C. M. Liaw, **"Establishment And Control Of A Three Phase Switched Reluctance Motor Drives Using Intelligent Power Modules."** *IET Electric Power Applications*, Vol. 4, Iss. 9, pp. 772-782, 2010.

[11] R. Krishnan**, "Switched Reluctance Motor Drives Modelling, Simulation, Analysis, Design and Applications."** Florida, U.S.A, CRC Press, 2001.

[12] M. Barnes and C. Pollock**, "Power Electronic Converters for Switched Reluctance Drives,"** *IEEE Transactions on Power Electronics*, Vol. 13, pp. 1100 – 1111, 1998.

[13] J. W. Ahn, J. Liang, and D. H. Lee, **"Classification and Analysis Of Switched Reluctance Converters,"** *Journal of Electrical Engineering and Technology*, Vol. 5, pp. 571 –579, 2010.

[14] Longya Xu, Jianrong Bu, **"Analysis of a Novel Converter Topology for Switched Reluctance Machine Drives,"** *International Conference on Power Electronic Drives and Energy Systems for Industrial Growth, Proceedings*, Vol. 2, pp. 640-645, 1998.

[15] R. Krishnan, A. M. Staley, K. Sitapati, **"A Novel Single-phase Switched Reluctance Motor Drive System,"** *Industrial Electronics Society, 2001. IECON '01. The 27th Annual Conference of the IEEE*, Vol. 2, pp. 1488- 1493, 2001.

[16] R. Krishnan, P. N. Materu, **"Design of A Single-Switch-Per-Phase Converter For Switched Reluctance Motor Drives,"** IEEE Transactions on Industrial Electronics, Vol. 37, Iss. 6, pp. 469-476, 1990.

[17] Omar Ellabban, Haitham Abu-Rub, **"Switched Reluctance Motors Converter Topologies: A Review,"** 2014 *IEEE International Conference on Industrial Technology.*, pp. 840-846, 2014.

[18] Vlad Petrus, **"Switched Reluctance Motors for Electric Vehicle Propulsion – Comparative Numerical and Experimental study of Control Schemes,"** PhD Dissertation, Dept. Electrical, Engineering., Univ. Libre de Bruxelles, Technical university of Cluj- Napoca, 2012.